Simulation verification analysis of anchoring characteristics of transverse rib steel bar during pull-out test

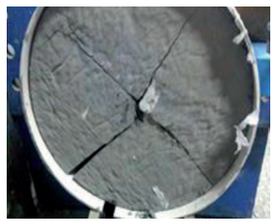

Análisis de la verificación por simulación de las características de anclado de barras de acero con entalla transversal durante el ensayo de extracción

Shuren Wang[1,2*], Huaiguang Xiao[2], Chen Cao[1,3], Zhengsheng Zou[1,2] and Xiliang Liu[1,2]

[1] Opening Laboratory for Deep Mine Construction, Henan Polytechnic University, Jiaozuo 454003, Henan, China
[2] School of Civil Engineering, Henan Polytechnic University, Jiaozuo 454003, Henan, China
[3] School of Civil, Mining and Environmental Engineering, University of Wollongong, Wollongong 2522, NSW, Australia
[*] E-mail: w_sr88@163.com

DOI: http://dx.doi.org/10.6036/8077 | Recibido: 06/04/2016 • Aceptado: 23/06/2016

RESUMEN

- Para evaluar las características mecánicas de anclado de una barra de acero con entalla transversal durante el ensayo de extracción, se llevaron a cabo diferentes métodos complementarios, como pruebas de laboratorio, simulación numérica y análisis teórico. Los resultados muestran que el bloque de anclado, durante el desarrollo de los ensayos de extracción, presenta un modo de fallo por agrietamiento y que la curva de relación fuerza de anclaje-desplazamiento, puede ser definida en cuatro pasos: fase de despegue, fase de avance, fase de agrietamiento y fase residual. Por eso la presentación analítica y las expresiones obtenidas para la curva de relación fuerza de anclaje-desplazamiento en los diferentes pasos se realizó usando un modelo de cilindro por elementos. Además, los resultados de la simulación numérica verificaron que el bloque cara a la entalla transversal desarrollaba la fuerza en forma de cuña y que se destruyó mostrando un modo de fractura por agrietamiento. Se encontró que la fuerza de anclaje y bloque residual cara a la entalla transversal aumentaban durante los ensayos de extracción con el incremento de la altura de la entalla. Estos resultados pueden facilitar una referencia básica para los diseños de refuerzo y la ingeniería práctica de construcción.
- **Palabras clave:** Ensayo de extracción, Barra con entalla transversal, Modelo de cilindro por elementos, Simulación numérica.

ABSTRACT

To evaluate the anchoring mechanical characteristics of transverse rib steel bar during the pull-out test, the comprehensive methods such as laboratory test, numerical simulation and theoretical analysis were conducted. The results show that the anchorage grout during the pull-out tests display the splitting failure mode and the relationship curve of anchorage force-displacement can be simplified into four stages: debonding stage, ascent stage, splitting stage, and residual stage. Then the analytical derivation and segregate expressions to the relationship curve of anchorage force-displacement at different stages were carried out by using the nested cylinder model. Furthermore, the numerical simulation results verified that the grout in front of the transverse rib presented the wedge-shape force and the anchorage grout displayed the splitting failure mode ultimately. It was found that the anchorage force and the remained grout in front of the transverse rib increase with the transverse rib height increasing during the pull-out tests. The results can provide a basic reference for the reinforcement design and safety construction of practice engineering.

Keywords: Pull-out test, Transverse rib bar, Nested cylinder model, Numerical simulation.

INTRODUCTION

The stress of steel bar in the reinforced concrete structure mainly depends on the bond anchorage effect between the steel bar and concrete, and the anchorage force of steel bar is the basis of the concrete structure. The engineering accidents of anchorage failure often occur owing to the loss of anchorage force of the steel bar. If the anchorage force is invalid, the bearing capacity of concrete structure is disabled, and the structure is destroyed. For anchoring theory lags the practice at present, it is of important theoretical significance and practical value to study the bearing performance of the pulled steel bar by using the methods such as laboratory experiments, numerical simulation, and theoretical analysis.

In recent years, there have been obtained lots of achievements about the anchorage mechanical property between the steel bar and bonding material. For examples, C. Li and B. Stillborg stated that both the bolt-grout interface and the rock-grout interface were easy to be destroyed in the rock anchor system, and the finally failure mode was depended on which interface was more weak during the pull-out test [1]. E. Hoek and D. F. Wood deemed that the bolt-grout interface was easier to be destroyed than other positions [2]. C. Cao et al. pointed out that it was very important to study the interaction mechanism in the rock anchor system [3]. S. Yazici and P. K. Kaiser proposed the bond strength model to analyze the bond of the bolt-grout interface, and the grout stress state could be divided into three stages: elastic stage, fully split stage, and partially split with an elastic portion stage [4]. C. R. Windsor regarded the fully-grouted bolt as continuously mechanically coupled system and carried out the anchorage mechanical property study [5]. J. H. Chen et al. investigated the shear stress distribution along the full length of the cable/grout interface when peak load occurring, they found that the non-uniform shear stress distribution along the interface was more apparent for cable bolts with long embedment length [6]. Y. C. Yin et al. studied the stress distribution evolution law and influencing factors along bolt anchorage segment by using laboratory tests and particle flow simulation [7]. Q. B. Wang et al. researched the complicated coupling effect between the anchorage force loss of anchor cable

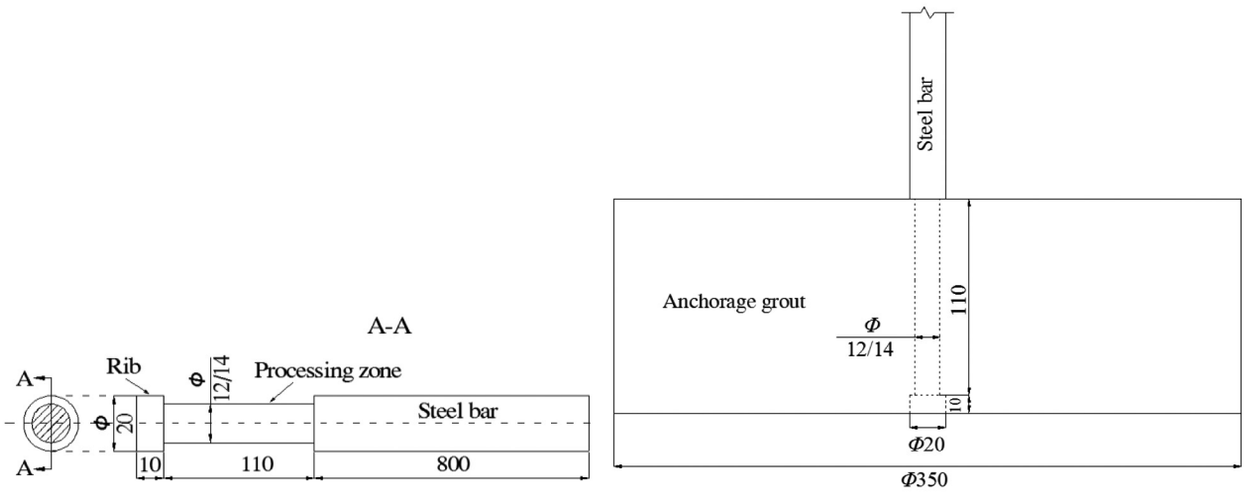

Fig. 1: Sizes of the rib bar and the test model (mm). (a) Sizes of the transverse rib bar; (b) Sizes of the test model

and rock or soil creep [8]. X. R. Liu et al. analyzed the pre-stress loss laws under different tensile and cyclic loads in field tests [9].

In terms of the anchoring force and displacement relationship, L. A. Lutz and P. Gergely obtained the shear and displacement relationship by using the pull-out test of the special signal rib bar [10]. S. Ma et al. proposed the shear stress distribution model of the bolt-grout interface, and deduced the anchorage force and displacement relationship for the fully-grouted bolts [11]. B. Benmokrane et al. analyzed the shear bond stress-slip relationship of the bolt-grout interface by using the tri-linear simplified model [12]. F. F. Ren et al. proposed that the full-range behavior of the bolt-grout interface consists of five consecutive stages: elastic stage, elastic-softening stage, elastic-softening-debonding stage, softening-debonding stage, and debonding stage. And they deduced the anchorage force-displacement relationship for each stage [13]. C. A. You deduced the formula of shear stress and axial force distribution along the axis direction of the fully-grouted bolts by using Mindlin's displacement solution [14]. M. H. Huang et al. established a non-liner differential equation of the anchorage segment load transfer and the non-liner shear slip model of the anchoring bolt based on the load-displacement curve. And they obtained the analytical solutions of shear stress and axial force behavior along the anchor rod [15]. W. P. Zhao et al. simulated the bond-slip relationship between steel bar and concrete by using ANSYS, and obtained the relationship curve of anchorage force-slip [16].

In a word, the above mentioned results mainly focused on the anchor force-displacement relations of the fully-grouted steel bar being pulled out from the anchorage body. This paper will analyze the anchorage mechanical property and anchorage force-displacement relationship during the transverse rib steel pull-out tests under the condition of the grout displaying the splitting mode. The remainder of this paper is organized as follows. Section 2 conducts the numerical and analytical analysis of anchorage performance of the transverse rib bar, respectively. Section 3 makes a discussion on the results. Section 4 summarizes the conclusions.

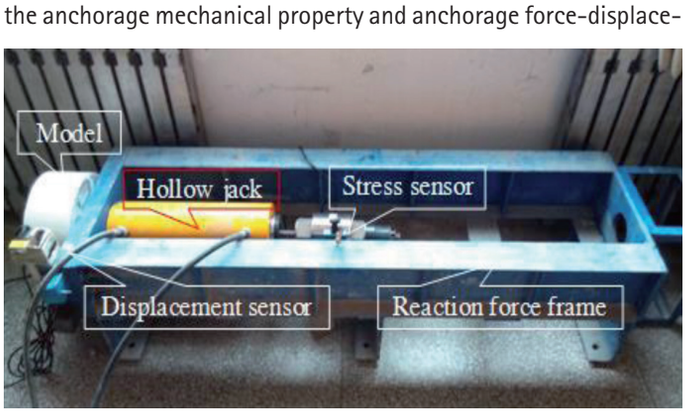

Fig. 2: Test equipment of the pull-out test

2. MATERIALS AND METHODS

2.1 SPECIMENTS AND TEST PROCESS

The basic materials in the pull-out test include the ordinary portland cement, HRB400 steel bar and PVC tube. As shown in Fig. 1(a), the transverse rib bar was made as the rib height 3.0 mm or 4.0 mm, respectively. The physical model of the anchorage grout was a cylinder, for which the diameter was 350 mm and the height was 120 mm (Fig. 1(b)). There were four specimens for different rig heights being tested in the laboratory, respectively.

The sensor of BL100-V-1000 was used to measure the displacement in the pull-out test and the electrical resistance strain pressure sensor of BLR-1/50t was used to monitor the axial force in the test, as shown in Fig. 2, and the eight-channel data acquisition system software of BL800-E8 was used to record the data of displacement and axial force in the test. According to the Building Anchor Bolt Test Method (China Code DG/TJ08-003-2000), the loading rate was 10 kN/min and the loading should be kept continuous and uniformly.

The test process was as follows: Firstly, the test specimen was fixed outside of the reaction force frame, and the loading device, the compressive and displacement sensors were set inside of the frame as shown in Fig. 2. Secondly, the steel bar was sequentially through the hole, the hollow jack and the compressive sensor, and the forepart of steel bar was fixed by the spherical anchorage. One end of the displacement monitoring was fixed to the frame, and the other end was fixed to the compressive sensor by the magnet. Thirdly, under the above mentioned conditions, when the anchorage force exceeded its maximum or the specimen was split completely, the loading test would be stopped.

2.2 NUMERICAL ANALYSIS OF ANCHORAGE PERFORMANCE

According to the test model in the laboratory (Fig. 1(b), the numerical computational model was built as shown in Fig. 3. To improve the computational efficiency, the computational model

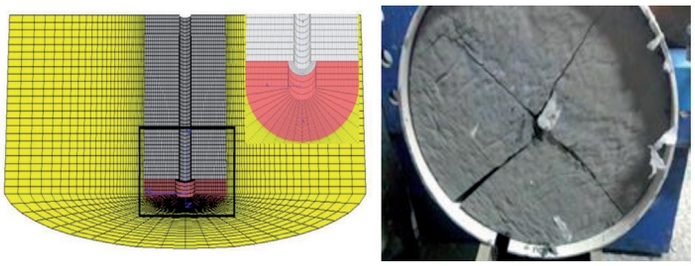

(a) (b)

Fig. 3: The computational model (a) and the radial distribution cracks of the grout (b)

was simplified the semi-cylinder model, and the diameter and the height of the model were 350 mm and 120 mm, respectively. The middle void of the model was the position of the anchorage steel bar. Since the anchorage steel bar was only affected by axial force, and the axial force only acted on the transverse rib, the steel bar axial force was equivalent to the transverse rib force, and the anchorage steel bar could be modeled by null model in FLAC^{3D}.

The out and top boundaries of the model were fixed, and the bottom boundary was free. The radial boundary of the steel bar in the middle void position of the model was fixed, and the axial boundary of the steel bar was free.

As shown in Fig. 3, the anchorage grout finally displayed the split failure mode when the transverse rib bar was pulled out during the pull-out test. It was supposed that the grout material conformed to the strain softening strength model in FLAC^{3D}. The mechanical parameters of the grout were listed in Table1.

In the numerical simulation test, a velocity was applied to the transverse rib plane of the model to simulate the pull-out force, and the axial displacement of the anchor steel bar and the maximum unbalanced force in front of transverse rib plane were recorded automatically. When the recorded anchorage force declined and showed the stable residue force, the numerical simulation was stopped.

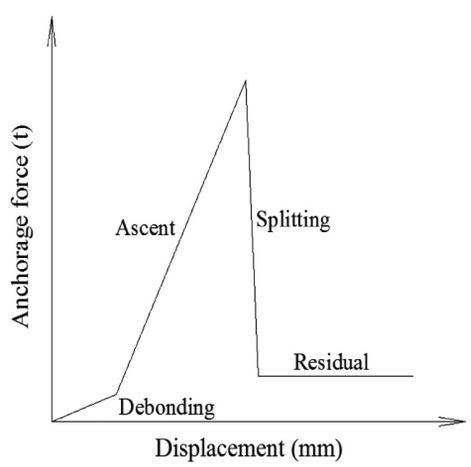

Fig. 4: The simplified anchorage force-displacement curve

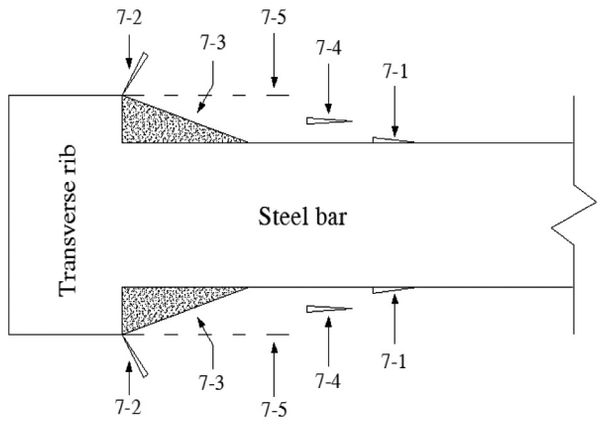

Fig. 5: The developing cracks in the pull-out test

2.3 ANALYTICAL EXPRESSION OF ANCHORAGE PERFORMANCE

As shown in Fig. 4, based on the laboratory test results, the anchorage force-displacement curve could be divided into four stages, such as debonding stage, ascent stage, splitting stage, and residual stage. The evolutionary process analysis of mechanical mechanism was shown in Fig. 5.

Debonding stage: with the load increasing in the pull-out test, the crack between the steel and the grout appeared and the local slipping emerged at step 7-1. With the load continuous increasing, the diagonal cracks of the top of the transverse rib appeared at step 7-2. In this stage, the anchorage force was small.

Ascent stage: with the load increasing and the local slipped interface developing, the grout in the front of the transverse rib displayed crushed damage and being piled into the wedge-shape mode to prevent from further slip at step 7-3. With the new slip interface appearing, the normal stress on the slip interface could be decomposed into normal stress and shear stress causing the longitudinal split cracks at step 7-4.

Splitting stage: with the longitudinal split cracks expanding, the grout in the front of the transverse rib being continuously further crushed, and after the anchorage force exceeding the maximum value, the longitudinal split cracks sharply expanded and then the anchorage force abruptly decreased at step 7-5.

Residual stage: the anchorage steel bar was pulled out, and the residual anchor force was smaller and basically remained stability.

In the pull-out test, it needed to be considered the steel bar strain how to influence on the axial slip displacement. The steel bar strain can be written in the form:

$$\varepsilon = \frac{\sigma}{E} \tag{1}$$

The steel bar stress is

$$\sigma = \frac{F}{S} \tag{2}$$

Name	Bulk modulus (GPa)	Shear modulus (GPa)	Cohesion (MPa)	Friction angle (°)	Tension (MPa)	UCS (MPa)
The actual grout	1.20	0.65	2.20	29	1.40	31.57
The simulated grout	1.20	0.65	2.20	29	1.40	
Steel bar	157.50	87.31			420	

Table 1: The mechanical parameters of the grout

And the circular section area of the steel bar is

$$S = \pi r^2 \tag{3}$$

where the radius r=0.01 m, and the elastic modulus E=210 GPa.

The maximum anchorage forces in Table 2 were put into the Formulas (1) to (3), and then the maximum strain e=4.6×10^{-4} of the steel bar could be calculated. Since the calculated strain compared with the displacement was very small, the calculated strain did not play a obvious affect on the axial slip displacement, so the steel bar could be regarded as a absolutely rigid material and it could not consume the internal works.

To simplify the analysis process, the anchorage force-displacement curve was divided into four stages, and each stage was analytical expressed.

No.	Water : cement	h (mm)	F (t)
1	0.4	4.0	3.03
2	0.4	3.0	2.60

Table 2: The maximum anchorage force in the pull-out tests

Debonding stage: before the new slip interface appearing, the formula of this stage was

$$F = k_1 u_{x1} \tag{4}$$

where $k_1 = \frac{5}{4\sqrt{h}}, u_{x1} \in (0, 0.8h)$, and h was the height of the transverse rib.

Ascent stage: as shown in Fig. 5, since the grout in front of the transverse rib was wedge-shape, the planar mechanical model (Fig. 6(a)), of this stage could be simplified as a nested cylinder model shown in Fig. 6(b). The confining pressure of the grout could be simplified as the uniformly distributed load to act on the transverse rib bar. Based on the energy theory, the steel bar pull-out force work was equal to the grout radial stress with the radial displacement work. The formula was

$$F u_{x2} = \sigma_r S u_r \tag{5}$$

In the pull-out test, the force of the transverse rib bar during before-and-after displacement was shown in Figs. 7(a) and 7(b). So the radial stress was

$$\sigma_r = K \cdot u_r \tag{6}$$

The radial stiffness was

$$K = \frac{E}{(1+\nu)a} = \frac{E}{(1+\nu)(r+u_r)} \tag{7}$$

The relationship between the radial displacement and the axial displacement is

$$u_r = u_{x2} \tan\alpha \tag{8}$$

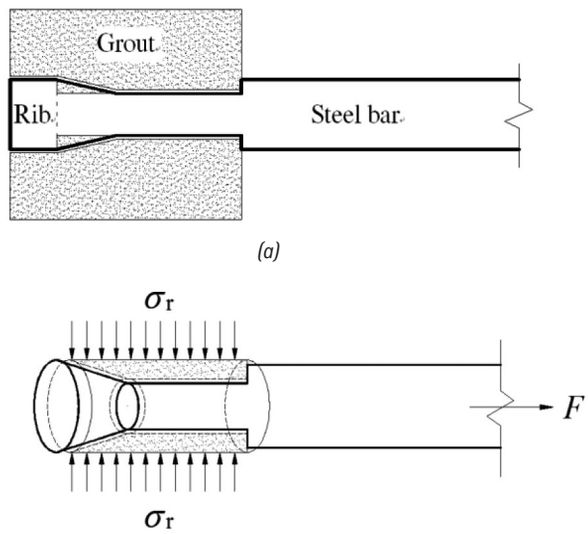

Fig. 6: The mechanical model and the nested cylinder model. (a) The mechanical model; (b) The nested cylinder model

The radial acted area caused by the radial displacement was

$$S = 2\pi(r+u_r)\left(\frac{h}{\tan\alpha}\right) \tag{9}$$

By formulas (5) to (9), it could be deduced the anchorage force F

$$F = \frac{E}{(1+\nu)(r+u_r)} u_r \cdot 2\pi(r+u_r)\left(\frac{h}{\tan\alpha}\right) \cdot \frac{u_r}{u_{x2}} = \frac{2\pi E h u_r}{1+\nu} = \frac{2\pi E h \tan\alpha}{1+\nu} u_{x2} \tag{10}$$

where $u_{x2} \in \left(0, \frac{12}{h}\right)$.

From the above deduced formulas, it was found that the anchorage force and the axial displacement had a liner relationship in the ascent stage. When the radial stress reached the maximum value, the grout displayed the splitting failure mode and the anchorage force reached the maximum value. The anchorage force was related to the rib height and the grout property.

Splitting stage: after the anchorage force reaches the maximum value, the anchorage force sharply declines and the anchorage capability was lost.

$$F = k_3 u_{x3} \tag{11}$$

where $k_3 = -0.9F_{max}, u_{x3} \in (0,1)$.

Residual stage: after the grout being split, the new slip interface appears and the residual anchorage force become very small.

$$F = t \tag{12}$$

where $t = 0.1F_{max}$.

3. RESULTS AND DISCUSSION

As shown in Fig. 8(a), both the laboratory test and the numerical simulation of the curve trends of the anchorage force-displacement relationships of the transverse rib bar (the rib height was 4.0 mm) were basic consistent. So the numerical simulation test was reliable. The anchorage force and the axial displacement relationship curves were shown in Fig. 8(b). It was found

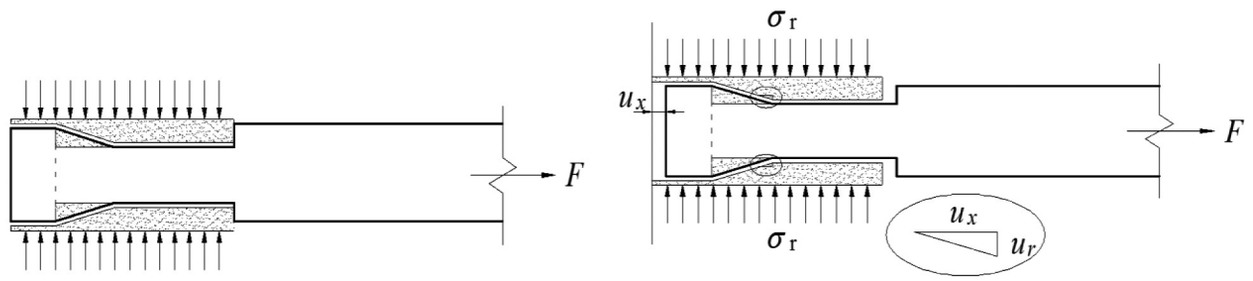

(a) (b)

Fig. 7: Comparative models before and after the pull-out test. (a) Before the pull-out test; (b) After the pull-out test

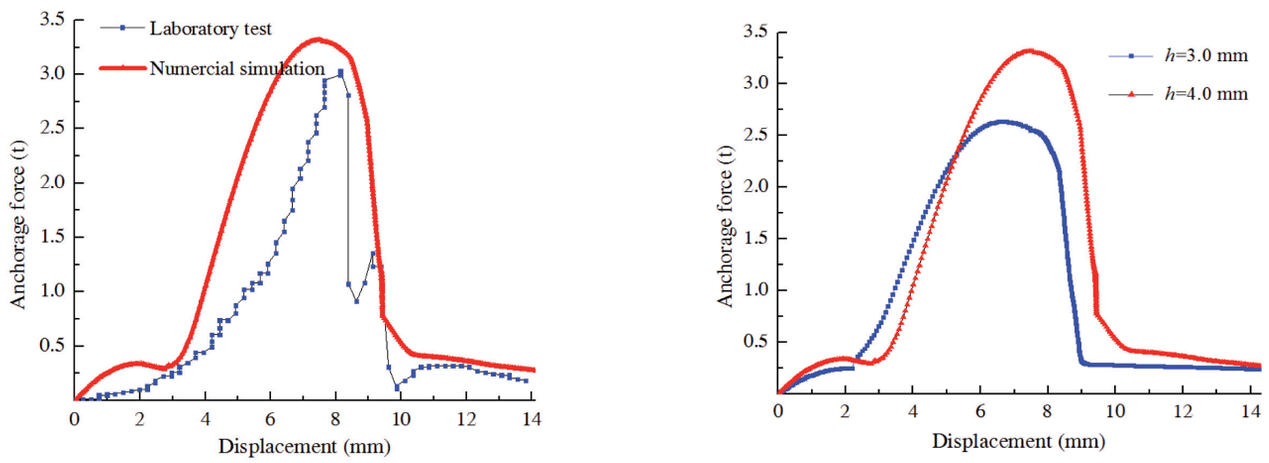

(a) (b)

Fig. 8: The anchorage force-displacement curves. (a) contrastive curves of test and simulation; (b) different rib heights

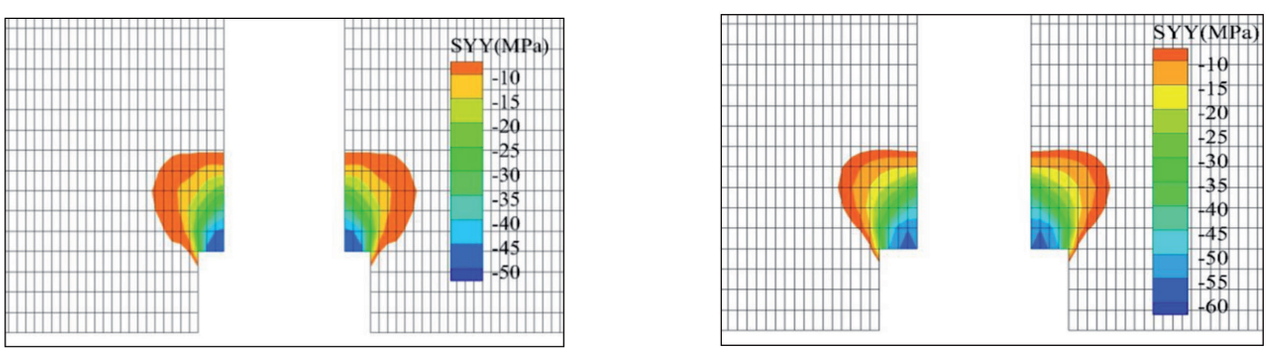

(a) (b)

Fig. 9: The axial stress contours under different rib heights. (a) h=3mm; (b) h=4mm

that the pull-out force first increased and then decreased with the axial displacement increased. When the pull-out force gradually reached the peak value, the axial displacement at ascent stage displayed a larger distance than that the pull-out force from peak value to the anchorage force losing at splitting stage. Compared two curves with different rib heights, it can be seen that the maximum anchorage force increased with the rib height increasing.

As shown in Fig. 9, the axial stress counters showed that the acted force on the grout in front of the transverse rib displaying wedge-shape. Compared Figs. 9(a) with 9(b), when the rib height was higher, the remained grout volume was lager and the compressive stress was also lager obviously.

According to the analytical expression of anchorage performance, submitting the grout elastic modulus E=1.60 GPa and the Passion's ratio n=0.3 into formula 10. When the rib height is 3.0 mm and 4.0 mm, the effective transverse angle is 16.7°, respectively. Thus, from formulas (4) to (12), the anchorage force-displacement curves can be obtained as shown in Fig. 10.

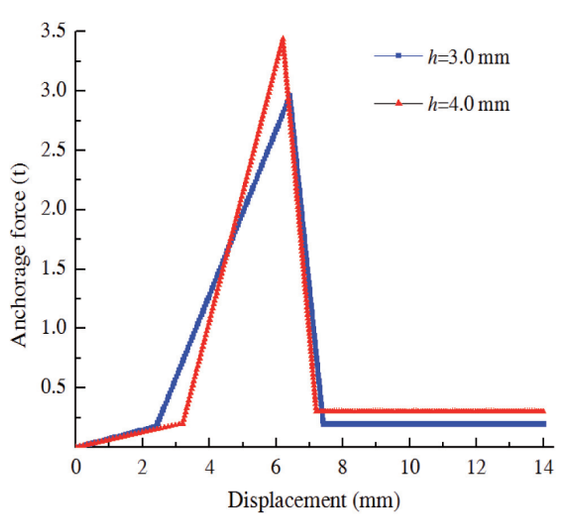

Fig. 10: Analytical expressions of anchorage force-displacement curves

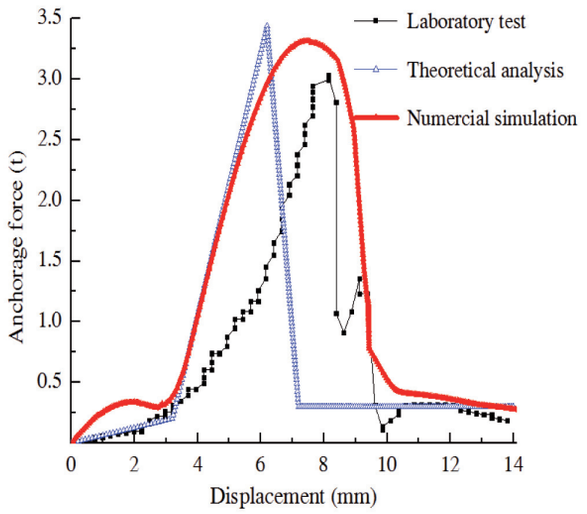

Fig. 11: The anchorage force-displacement curves under different conditions

As shown in Fig. 11, through the pull-out tests (the transverse rib height was 4.0 mm), the three types curves (laboratory test, theoretical analysis, and numerical simulation) of anchorage force-displacement were obtained, the segmentation of each curve was obvious and the curve deformation trends of three types were basically consistent. Namely, with the displacement increasing, the anchorage force first increased and then decreased. Since the grout material was supposed conforming to the strain softening strength model in numerical simulation, the anchorage force gradually reached the peak value, and the grout displayed gradual softening not splitting sharply, so the displacement became lager. In addition, the transverse rib bar was regarded as absolutely rigid material in the theory analysis, so the displacement was relatively small and the anchorage force peak value was relatively large.

In the pull-out test of the transverse rib bar, with the displacement increasing, the anchorage force first increased and then decreased under the grout displaying the splitting failure mode. Before the anchorage force reaching the peak value, the axial displacement was large, and when the anchorage force reached the peak value until to losing the anchorage force, the axial displacement was smaller. S. M. Mirza and J. Houde stated that the anchorage force-displacement relationship curve first increased and then decreased by conducting many pull-out tests.

This deformation tendency is consistent with the results in this paper [17]. In this paper, since there was not the confining pressure being acted on the grout out boudaries, when the anchorage force reached the peak value, the anchorage force declined sharply and the anchorage capability was lost quickly.

4. CONCLUSIONS

Based on the laboratory tests, the anchorage force-displacement relationship curves can be simplified four stages, such as debonding stage, ascent stage, split stage, and residual stage. And the axial displacement in the ascent stage was larger than that in the split stage.

According to the anchorage force-displacement relationship curves, these analytical expressions to four stages were carried out and the maximum anchorage force formula was deduced by using the nested cylinder model.

The numerical simulation results verified that the anchorage force and the remained grout volume in front of the transverse rib increased with the transverse rib height increasing. The results are of reference significance for the steel bar with similar ribs in reinforcement design and safety construction of practice engineering.

BIBLIOGRAPHY

[1] Li C, Stillborg B. "Analytical models for rock bolts". International Journal of Rock Mechanics & Mining Sciences. December 1999. Vol. 36-8. p. 1013-1029. DOI: http://dx.doi.org/10.1016/S1365-1609(99)00064-7
[2] Hoek E, Wood D F. "Rock support". World Tunnlg. April 1989. Vol. 2-2. p. 131-136.
[3] Cao C, Ren T, Cook C, et al. "Analytical approach in optimising selection of rebar bolts in preventing rock bolting failure". International Journal of Rock Mechanics & Mining Sciences. December 2014. Vol. 72. p. 16-25. DOI: http://dx.doi.org/10.1016/j.ijrmms.2014.04.026
[4] Yazici S, Kaiser P K. "Bond strength of grouted cable bolts". International Journal of Rock Mechanics & Mining Sciences & Geomechanics Abstracts. May 1992. Vol. 29-3. p. 279-292. DOI: http://dx.doi.org/10.1016/0148-9062(92)93661-3
[5] Windsor C R. "Rock reinforcement systems". International Journal of Rock Mechanics & Mining Sciences. September 1997. Vol. 34-6. p. 919-951. DOI: http://dx.doi.org/10.1016/S1365-1609(97)80004-4
[6] Chen J H, Saydam S, Hagan P C. "An analytical model of the load transfer behavior of fully grouted cable bolts". Construction and Building Materials. December 2015. Vol. 101-1. p. 1006-1015. DOI: http://dx.doi.org/10.1016/j.conbuildmat.2015.10.099
[7] Yin Y C, Zhao T B, Tan Y L, et al. "Research of stress distribution evolution law and influencing factors". Journal of Mining & Safety Engineering. October 2013. Vol. 30-5. p. 712-716.
[8] Wang Q B, Zhang G, Wang H, et al. "Study of coupling effect between anchorage force loss of prestressed anchor cable and rock and soil creep". Rock and Soil Mechanics. August 2014. Vol. 35-8. p. 2150-2156.
[9] Liu X R, Liu Y Q, Kang J W, et al. "Prestress loss laws of anchor cables in foundation pits and control measures of tension by steps". Chinese Journal of Geotechnical Engineering. October 2015. Vol. 37-10. p. 1794-1801.
[10] Lutz L A, Gergely P. "Mechanics of bond and slip of deformed bars in concrete". Am Concrete Inst Journal & Proceedings. November 1967. Vol. 64-11. p. 711-721.
[11] Ma S, Nemcik J, Aziz N. "An analytical model of fully grouted rock bolts subjected to tensile load". Construction & Building Materials. December 2013. Vol. 49-1. p. 519-526. DOI: http://dx.doi.org/10.1016/j.conbuildmat.2013.08.084
[12] Benmokrane B, Chennouf A, Mitri H S. "Laboratory evaluation of cement-based grouts and grouted rock anchors". International Journal of Rock Mechanics and Mining Sciences & Geomechanics Abstracts. October 1995. Vol. 32. p. 633-642. DOI: http://dx.doi.org/10.1016/0148-9062(95)00021-8
[13] Ren F F, Yang Z J, Chen J F, et al. "An analytical analysis of the full-range behavior of grouted rockbolts based on a tri-linear bond-slip model". Construction & Building Materials. March 2010. Vol. 24-3. p. 361-370. DOI: http://dx.doi.org/10.1016/j.conbuildmat.2009.08.021
[14] You C A. "Mechanical analysis on wholly grouted anchor". Chinese Journal of Rock Mechanics and Engineering. March 2000. Vol. 19-3. p. 339-341.
[15] Huang M H, Zhou Z, Ou J P. "Nonlinear analysis on load transfer mechanism of wholly grouted anchor rod along anchoring section". Chinese Journal of Rock Mechanics and Engineering. August 2014. Vol. 33(S2). p. 3992-3997. DOI: http://dx.doi.org/10.13722/j.cnki.jrme.2014.s2.076
[16] Zhao W P, Fan Y H, Li G. "Numerical simulation of bond-slip between HSC and steel bar". Journal of Lanzhou Jiaotong University. December 2010. Vol. 29-6. p. 20-24. DOI: http://dx.doi.org/10.3969/j.issn.1001-4373.2010.06.005
[17] Mirza S M, Houde J. "Study of bond stress-slip relationships in reinforced-concrete". Journal of the American Concrete Institute. January 1979. Vol. 76-1. p. 19-46.

ACKNOWLEDGEMENTS

This work was supported by the National Natural Science Foundation of China (51474188; 51474097; 51074140), the Natural Science Foundation of Hebei Province of China (E2014203012), the International Cooperation Project of Henan Science and Technology Department (162102410027), the Doctoral Fund of Henan Polytechnic University (B2015-67), and Program for Taihang Scholars. All these were gratefully acknowledged.